RSC Advances

ROYAL SOCIETY OF CHEMISTRY

PAPER

View Article Online
View Journal | View Issue

Cite this: *RSC Adv.*, 2023, **13**, 36035

Chalcone Mannich base derivatives: synthesis, antimalarial activities against *Plasmodium knowlesi*, and molecular docking analysis†

Jufrizal Syahri,*[a] Rahmiwati Hilma,[a] Amatul Hamizah Ali,[b] Norzila Ismail,[c] Ng Yee Ling,[d] Nurlaili,[a] Beta Achromi Nurohmah,[e] Hani Kartini Agustar,[f] Lau Yee Ling[d] and Jalifah Latip*[b]

Development and discovery of new antimalarial drugs are needed to overcome the multi-resistance of *Plasmodium* parasites to commercially available drugs. Modifying the substitutions on the amine groups has been shown to increase antimalarial activities and decrease cross-resistance with chloroquine. In this study, we have synthesized several chalcone derivatives *via* the substitution of aminoalkyl groups into the aromatic chalcone ring using the Mannich-type reaction. The chalcone derivatives were evaluated for their antimalarial properties against *Plasmodium knowlesi* A1H1 and *P. falciparum* 3D7, as well as their molecular docking on *Plasmodium falciparum* dihydrofolate reductases-thymidylate synthase (PfDHFR-TS). Data from *in vitro* evaluation showed that chalcone Mannich-type base derivatives **2a**, **2e**, and **2h** displayed potential antimalarial activities against *P. knowlesi* with EC_{50} of 2.64, 2.98, and 0.10 μM, respectively, and *P. falciparum* 3D7 with EC_{50} of 0.08, 2.69, and 0.15 μM, respectively. The synthesized compounds **2a**, **2e**, and **2h** exerted high selectivity index (SI > 10) values on the A1H1 and 3D7 strains. The molecular docking analysis on PfDHFR-TS supported the *in vitro* assay of **2a**, **2e**, and **2h** by displaying CDOCKER energy of −48.224, −43.292, and −45.851 kcal mol^{-1}. Therefore, the evidence obtained here supports that PfDHFR-TS is a putative molecular target for the synthesized compound.

Received 7th August 2023
Accepted 4th December 2023

DOI: 10.1039/d3ra05361j

rsc.li/rsc-advances

Introduction

Malaria is an infectious disease caused by protozoa parasites of the genus *Plasmodium* like *P. falciparum* and *P. knowlesi*, which can be transmitted through the bite of the female *Anopheles* spp. mosquito. According to the World Health Organization (WHO), malaria cases reached 247 million and approximately 619 000 malaria deaths occurred globally in 2021. Southeast Asia has the second highest cases of malaria globally.[1,2] The high incidence rate of *P. falciparum* in Southeast Asia countries is expected due to gene mutation in the parasite which develops resistance to major antimalarial drugs such as chloroquine, artemisinin, and several new antimalarial compounds such as dihydroisoquinolones, spiroindolones, and pyrazoles.[3–5] Although many studies have been conducted to assess the effectiveness of artemisinin derivatives[6] as antimalarial agents, it is notable that *N*-sulfonylpiperidinedispiro-1,2,4,5-tetraoxane analogs demonstrate promising antimalarial properties during *in vivo* evaluations.[7] Dispiro-tetraoxanes, synthetic peroxides, known for their efficacy against drug-resistant *P. falciparum*, have been discussed by Yadav *et al.*[8] A significant drawback of relying on artemisinin derivatives as a sole treatment is the heightened occurrence of late-stage parasite recrudescence.[4] Hence, exploring a single class of drugs with a specific mechanism of action to prevent mutation is insufficient in addressing malarial infection.

One gene mutation that commonly occurs is at dihydrofolate reductase-thymidylate synthase of *Plasmodium falciparum* (PfDHFR-TS), a well-known target for the antifolate drugs such as pyrimethamine and cycloguanil. The targeted gene is crucial to produce folates and thymidylate (dTMP) required for DNA synthesis in the malarial parasite.[9] The emergence of antifolate resistance in PfDHFR-TS is an urgent issue that needs to be encountered for antimalarial medication. Therefore, the rise in malaria cases linked to *P. falciparum* resistance highlights the

[a]*Department of Chemistry, Universitas Muhammadiyah Riau, Jalan Tuanku Tambusai Ujung, Pekanbaru, Indonesia. E-mail: jsyachri@umri.ac.id*

[b]*Department of Chemical Sciences, Faculty of Science and Technology, Universiti Kebangsaan Malaysia, 43600 UKM Bangi, Selangor, Malaysia. E-mail: jalifah@ukm.edu.my*

[c]*Department of Pharmacology, School of Medical Sciences, Universiti Sains Malaysia, 16150 Kubang Kerian, Kelantan, Malaysia*

[d]*Department of Parasitology, Faculty of Medicine, Universiti Malaya, 50603, Kuala Lumpur, Malaysia*

[e]*Department of Chemistry, Universitas Gadjah Mada, Jalan Kaliurang Sekip Utara Bulaksumur 21, 55281, Yogyakarta, Indonesia*

[f]*Department of Earth Science and Environment, Faculty of Science and Technology, Universiti Kebangsaan Malaysia, 43600 UKM Bangi, Selangor, Malaysia*

† Electronic supplementary information (ESI) available. See DOI: https://doi.org/10.1039/d3ra05361j

importance of continual research, especially the heightened emphasis on discovering novel antimalarial drugs.

Chalcone is one of the natural compounds that are active as an antimalarial.[10–12] The activity of the chalcone compound comes from the functional groups attached to the aromatic ring and the alpha–beta unsaturated ketone bridge that connects the two rings. The alpha–beta unsaturated ketone moiety in chalcone is considered a Michael acceptor. This conjugated double bond makes chalcone compounds have a mechanism for electron transfer. These properties also make chalcone-derived compounds possess many activities, such as antimalarial[13–16] (Fig. 1), anticancer,[17–19] anti-inflammatory,[20,21] antibacterial,[22–24] antioxidants,[25,26] antidiabetic,[27,28] antigiardial,[29] and antileukemic.[30] Chalcone derivatives with a substituent secondary amine group could be proposed to increase the antimalarial activity.[31,32]

In the study of Structure–Activity Relationship (SAR) analysis, it is known that most of the commercially available antimalarial drugs contain the amine group.[33] This fact justifies that the amine group plays an important role in antimalarial activity. According to Suwito *et al.*,[13] amines can form electrostatic interactions with carbonyl groups in a protein of the *Plasmodium* parasite, which can kill the parasite.[13] In our previous study, adding aminoalkylated such as morpholine, piperidine, and diethylamine on chalcone significantly enhanced the antimalarial activity with IC_{50} values in a range of 0.54 to 1.12 μM against *P. falciparum* 3D7, compared with the chalcone without amine group.[34] A prenylated and allylated chalcone showed the best IC_{50} values of 1.08 and 1.73 μg mL^{-1}, respectively against the *P. falciparum* 3D7 strain.[14] In addition, we previously synthesized and assessed a series of chalcone derivatives in which one of them substituted with the piperidine moiety showed an IC_{50} value of 0.54 μM and was categorized as having potential antiplasmodial candidate.[32]

In this study, the substitution of aminoalkyl groups into the aromatic chalcone ring was prepared using the Mannich-type reaction and studied for the first time against *P. knowlesi* and *P. falciparum*. The aminoalkyl groups used are piperidine, methyl piperidine, morpholine, and dimethylamine. All chalcone Mannich-type base derivatives were tested for drug susceptibility test against the zoonotic parasite *P. knowlesi*, and non-zoonotic parasite *P. falciparum in vitro* evaluation and followed by molecular docking on PfDHFR-TS and ADMET analyses. We proposed that the presence of an amine group could increase the antimalarial activity of the chalcone compounds. The present study is crucial to obtain insights into the crucial role of the amine group in chalcone derivatives to prevent the emergence of antifolate resistance and malarial transmission.

Results and discussion

Synthesis of aminoalkylated chalcone derivatives

The prepared chalcones **1(a–d)** were obtained in a good yield *via* Claisen–Schmidt aldol condensation. Meanwhile, we also successfully synthesized the aminoalkylated-chalcones **2(a–h)** from chalcone **1(a–d)** by term Mannich-type reaction to substitute some aminoalkyl groups (Fig. 2). The spectroscopy analysis (^{1}H-NMR, ^{13}C-NMR, and MS) defined the structure of the desired products. The chemical structures of the synthesized derivatives are depicted in Fig. 3.

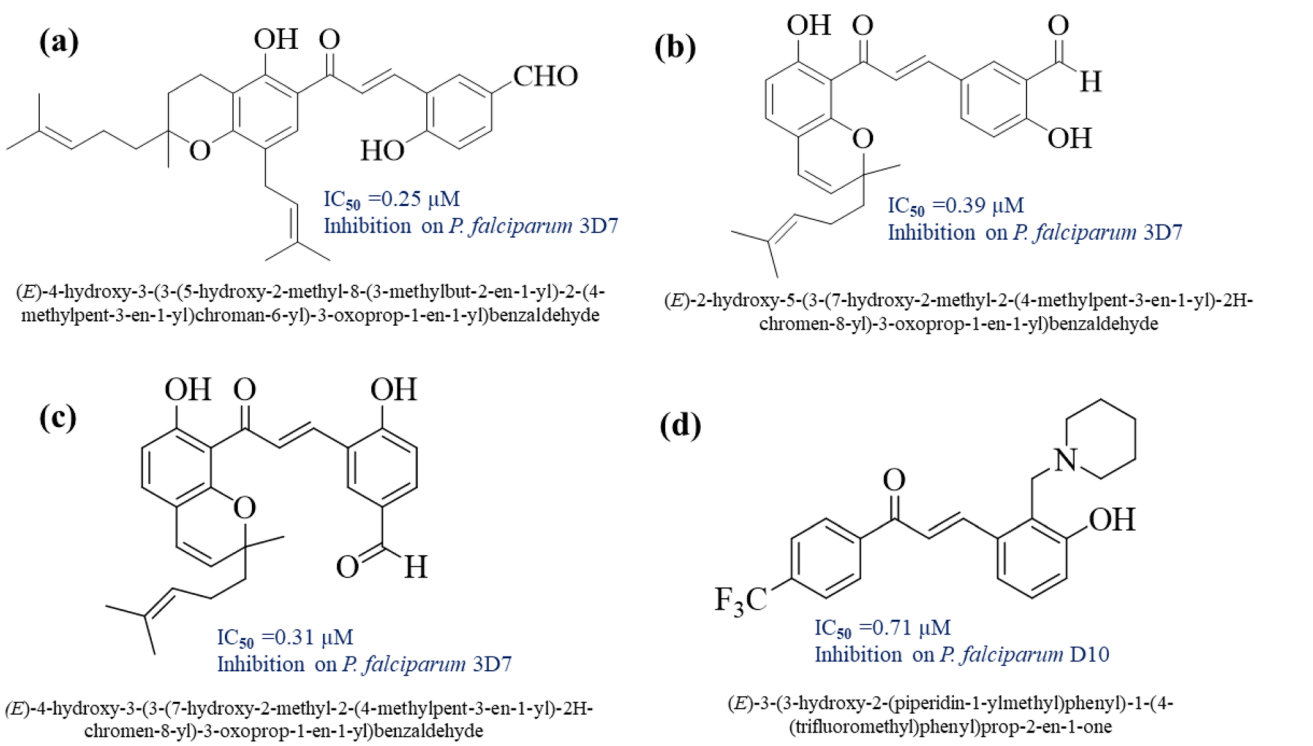

Fig. 1 Chalcone derivatives possessed antimalarial properties.[15,18]

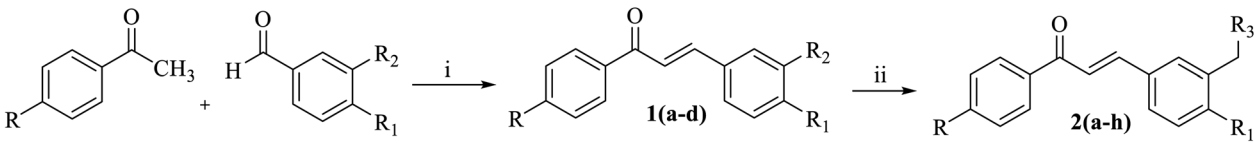

Fig. 2 Reaction scheme of aminoalkylated chalcones derivatives **1(a–d)** and **2(a–h)** from substituted-benzaldehyde and substituted-acetophenone. (i) Kalium hydroxide (60%), ethanol, stir at room temperature (RT) overnight; (ii) aminoalkyl groups, formaldehyde, ethanol, stir for 20 hours. R, R1, R2 = functional group from aldehyde and ketone; R3 = aminoalkyl groups.

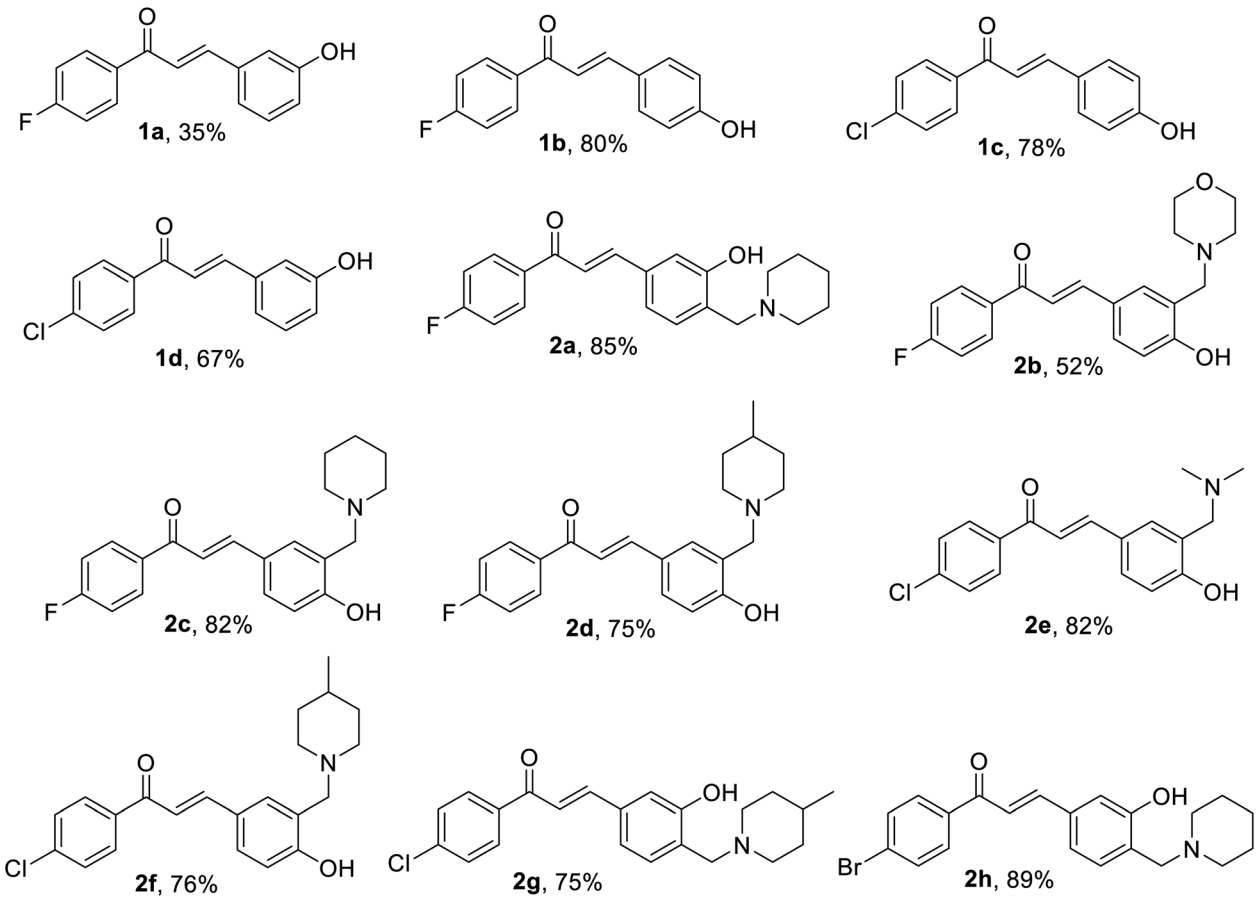

Fig. 3 Molecular structures of synthesized chalcones (**1a–1d**, yield in %) and aminoalkylated chalcones derivatives (**2a–2h**, yield in %).

Antimalarial activities against *P. knowlesi* A1H1 and *P. falciparum* 3D7

The *in vitro* antimalarial activity assay was performed against the *P. knowlesi* A1H1 and *P. falciparum* 3D7 strains using *Plasmodium* lactate dehydrogenase assay (pLDH). The findings in EC_{50} values (μM) against the *P. knowlesi* A1H1 and *P. falciparum* 3D7 are presented in Table 1. Based on the result in Table 1, from 12 synthesized derivatives, chalcone derivatives **2h** possessed potent parasite inhibition against *P. knowlesi* A1H1 with the EC_{50} value in micromolar concentration (0.10 μM) as compared to other compounds. Chalcone derivatives **2a**, **2d**, **2e**, and **2f** exhibited active inhibition against the A1H1 strain with EC_{50} values of 2.64, 11.98, 2.98, and 19.91 μM respectively. The other seven chalcone derivatives were determined to have moderate antimalarial activities against the A1H1 strain. In addition, chalcone derivatives **2a** and **2h** were classified to have potential antimalarial activities with EC_{50} of 0.08 and 0.15 μM, respectively against *P. falciparum* 3D7, while **2d**, **2e**, and **2f** exerted good antimalarial activities with EC_{50} values of 5.97, 2.69, and 17.03 μM respectively. The other synthesized chalcone derivatives gave moderate parasite inhibitory effects against the 3D7 strain. The antimalarial threshold activities are determined as follows, EC_{50} < 1 μM as potential activity, 2–20 μM as active/good activity, 21–100 μM as moderate activity, 101–200 as weak activity, and EC_{50} > 201 as inactive.[34–36] The EC_{50} values for the reference antimalarial drug, chloroquine diphosphate (CQ) 0.04 μM for *P. knowlesi* A1H1 and 0.0018 μM for *P. falciparum* 3D7 in line with its usage as the frontline drug for treating malarial infection. The EC_{50} value of **2a** against the A1H1 strain was about 66-fold higher than CQ, while the EC_{50} value of **2a** against

Table 1 Antimalarial and cytotoxic activities of chalcone Mannich-type base derivatives[a]

Test compound	*P. knowlesi* A1H1 (CQ-sensitive) EC_{50} (μM) ± SD	*P. falciparum* 3D7 (CQ-sensitive) EC_{50} (μM) ± SD	WRL-68 cell (mammalian cell) IC_{50} (μM) ± SD	Selectivity index (SI), $\left(\frac{IC_{50}\ MTT}{EC_{50}\ pLDH}\right)$	
				P. knowlesi	*P. falciparum*
1a	29.00 ± 0.61	26.07 ± 0.03	38.94 ± 8.01	1.34	1.50
1b	78.91 ± 0.36	>41.28	11.10 ± 7.97	0.14	0.27
1c	35.53 ± 3.88	>38.66	18.50 ± 6.40	0.52	0.48
1d	36.84 ± 6.27	>38.66	11.44 ± 7.04	0.31	0.30
2a	2.64 ± 1.74	0.08 ± 0.01	27.65 ± 6.47	10.50	345.63
2b	24.64 ± 3.94	>29.29	16.13 ± 6.76	0.65	0.55
2c	21.06 ± 2.12	>29.46	22.94 ± 5.97	1.09	0.78
2d	11.98 ± 0.66	5.97 ± 0.02	10.37 ± 7.64	0.89	1.74
2e	2.98 ± 0.14	2.69 ± 0.02	138.34 ± 7.81	46.42	51.42
2f	19.91 ± 2.11	17.04 ± 0.02	80.65 ± 7.19	4.10	4.73
2g	31.84 ± 0.30	27.54 ± 0.23	14.76 ± 6.37	0.47	0.54
2h	0.10 ± 0.05	0.15 ± 0.03	>99.00	990	660
CQ	0.04 ± 0.001	0.0018 ± 0.0008	102.82 ± 0.24	>2500	>2500

[a] CQ: chloroquine diphosphate, EC_{50}: half-maximal effective concentration, IC_{50}: half-maximal inhibition concentration, SD: standard deviation, nd: not determined.

3D7 was about 48-fold higher than CQ. In addition, the EC_{50} value of **2e** against the A1H1 strain was about 75-fold higher than CQ, while the EC_{50} value of **2e** against 3D7 was about 1400-fold higher than CQ. A high potency of **2h** was seen as the EC_{50} value against A1H1 was about 3-fold higher than CQ, and 83-fold higher than CQ in 3D7 infection. Thus, chalcone derivatives **2a**, **2e**, and **2h** possessed promising antimalarial activities against A1H1 and 3D7 strains.

Structural-based analysis was also performed to determine the best substituents in chalcone derivatives that give the best candidate as antimalarial. In these findings, we postulated that the addition of an aminoalkyl group to chalcone could increase antimalarial efficacy. The addition of aminoalkyl groups such as piperidine, methyl piperidine, and diethylamine was proposed could increase antimalarial activity as discovered in this study. This can be seen from the presence of piperidine moiety in chalcone derivative **2a** which has better antimalarial activity (EC_{50} of 0.08 μM) against *P. falciparum* 3D7 than compound **1a** (EC_{50} of 26.06 μM). Similarly, the addition of the aminoalkyl group, dimethylamine in chalcone derivative **2e** increased the antimalarial activity from chalcone derivative **1c** with a reduction in EC_{50} value from 38.66 to 2.69 μM can be observed. In addition, the antimalarial effect can be better identified in chalcone derivative **2a** (with piperidine moiety) against *P. knowlesi* A1H1 compared to **1a**, which showed a lower EC_{50} value was observed in chalcone derivative **2a** (2.64 μM). The addition of the aminoalkyl group, dimethylamine in chalcone derivative **2e** also affected the antimalarial efficacy by lowering the EC_{50} value of chalcone derivative **1c** from 35.5 to 2.98 μM (**2e**). The addition of piperidine moiety and bromide in chalcone derivative **2h** enhanced the antimalarial efficacy of the compound against *P. knowlesi* A1H1 and *P. falciparum* 3D7. Thus, this result indicates that the aminoalkyl group does play a very important role in the antimalarial activity.

Cytotoxic activities against WRL-68 mammalian cells and selectivity indexes

The findings of the cytotoxicity assay (MTT) against the WRL-68 mammalian cell line revealed that all twelve chalcone derivatives did not show any strong toxicity effect *in vitro* (Table 1). The IC_{50} values of all compounds were determined in the range of 10 to 80 μM, suggesting the compounds were moderately toxic to the cell line. Chalcone derivatives **2e** and **2h** were considered non-toxic with IC_{50} more than 100 μM. The threshold level for cytotoxic effect was referred to as compounds with IC_{50} values lower than 10 μM were classified as highly toxic to mammalian cells.[37,38] Based on the cytotoxic and antimalarial data, we further calculated the selectivity indexes (SI) of the chalcone derivatives to test the efficacy of the synthesized compounds as antimalarials and their pharmacological properties as safe drugs. For *in vitro* evaluation against *P. knowlesi* A1H1, chalcone derivatives **2a**, **2e**, and **2h** exerted SI values of more than 10. The high SI values (SI = 10 to 990) shown by these compounds explained the antimalarial efficacy of these compounds as selective inhibition toward the *P. knowlesi* A1H1. In addition, for *in vitro* assessment against *P. falciparum* 3D7, **2a**, **2e**, and **2h** had SI values greater than 10 (SI = 51 to 660), indicating that their pharmacological potential exceeded that of selective and safe drugs. Other compounds exhibited low SI

Table 2 Computational prediction of CDOCKER energy (kcal mol^{-1}) of chalcone derivatives (**2a**, **2e**, and **2h**) on PfDHFR-TS

Compounds	CDOCKER energy (kcal mol^{-1})	Hydrogen-bonding
2a	−48.224	Ile164, Ala16, Cys15, Ser108, Gly166
2e	−43.292	Ile164, Ala16, Cys15, Tyr170
2h	−45.851	Ile164, Tyr170, Ser111, Ile112

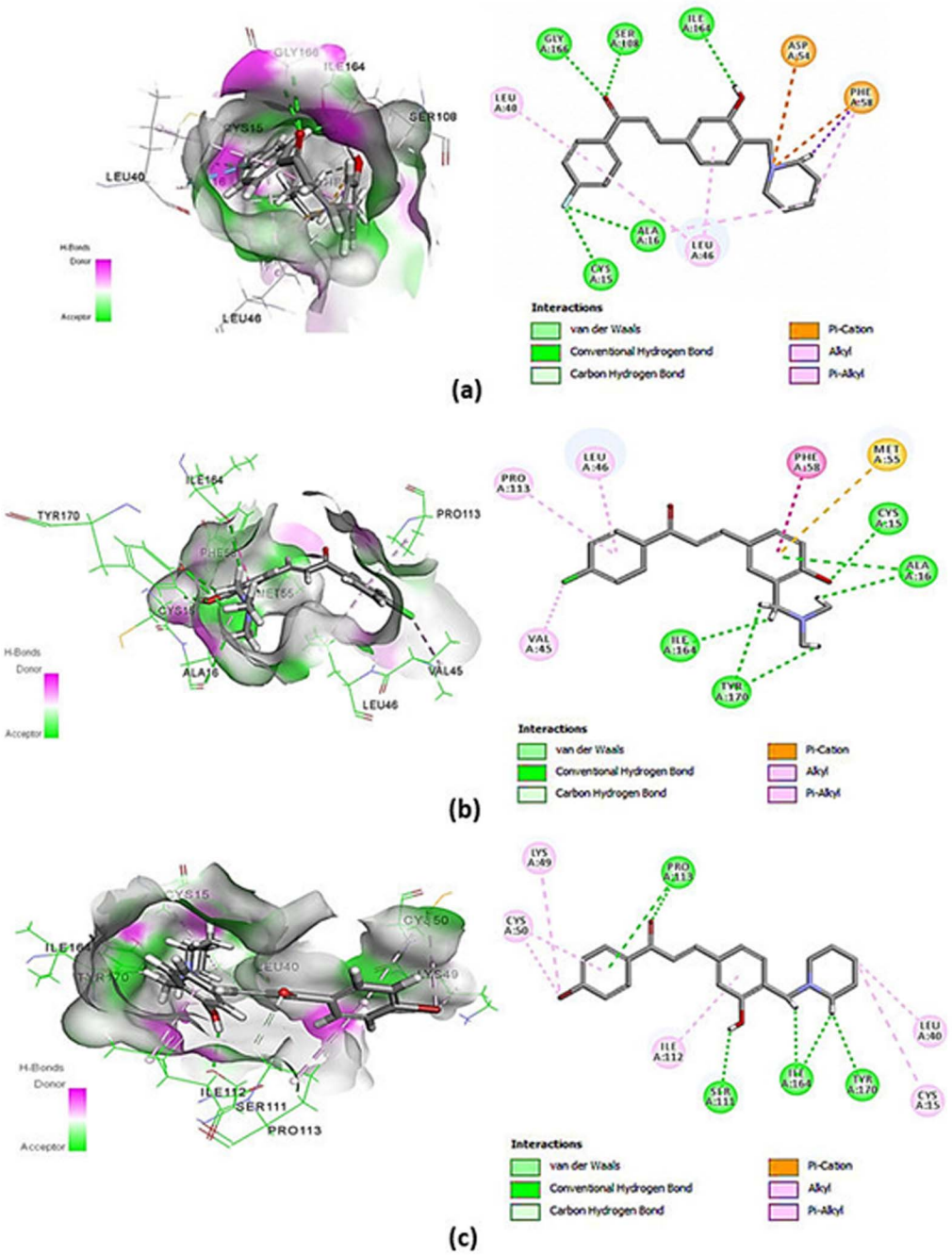

Fig. 4 Visualization of the interaction (2-dimensional and 3-dimensional) among (a) chalcone derivative **2a**, (b) chalcone derivative **2e**, and (c) chalcone derivative **2h** with PfDHFR-TS. The atom coloring scheme is as follows: carbons in grey, oxygen in red, and nitrogen in blue. Green lines represent hydrogen-bonding interactions, while the pink line represents π-bonding interactions.

values (SI < 10) indicating that the compounds had higher cytotoxic properties and lower parasite inhibition effect as compared to **2a**, **2e**, and **2h**. The antimalarial properties of **2a**, **2e**, and **2h** are almost comparable for both parasite strains. This might be caused by both parasite strains being sensitive strains that do not develop into multidrug-resistant varieties.

From all tested chalcone derivatives, we would like to suggest **2a**, **2e**, and **2h** are the most promising antimalarial candidate against both the zoonotic parasite, *P. knowlesi*, and non-zoonotic parasite, *P. falciparum* due to their active inhibition of both strains according to their low EC_{50} antimalarial values, high IC_{50} cytotoxic values as well as high SI values. These findings are in accordance with our postulation that the addition of an aminoalkyl group to chalcone could increase the parasite inhibitory effect. The presence of piperidine moiety in chalcone derivatives **2a**, and **2h**, and the addition of the aminoalkyl group, dimethylamine in chalcone derivative **2e** increased the antimalarial activities of both compounds against

P. knowlesi and *P. falciparum*. These findings further justify that the substitution of the amine group in chalcone derivatives could enhance the antimalarial efficacy of the compounds. A series of synthesized chalcone derivatives in our previous study such as chalcone derivatives added with morpholine, diethylamine, and piperidine moieties produced almost similar parasite inhibitory effect against *P. falciparum* 3D7.[11,32,33] However, the antimalarial properties of (*E*)-1-(4-fluorophenyl)-3-(3-hydroxy-4-(piperidin-1-ylmethyl)phenyl)prop-2-en-1-one (**2a**), (*E*)-1-(4-chlorophenyl)-3-(3-dimethylamino)-(4-hydroxyphenyl) prop-2-en-1-one (**2e**), and (*E*)-1-(4-bromophenyl)-3-(3-hydroxy-4-(piperidin-1-ylmethyl)phenyl)prop-2-en-1-one (**2h**) against *P. knowlesi*, and *P. falciparum* are the first report so far.

Molecular docking analysis

The molecular docking result showed that chalcones **2a**, **2e**, and **2h** have CDOCKER energy of −48.224, −43.292, and −45.851 kcal mol^{-1} (Table 2) (Fig. 4a–c), apparently higher than the co-crystal inhibitor WR9910 with −54.320 kcal mol^{-1}.[39] The re-docking process of the PfDHFR-TS–WR99210 complex showed interaction with Ala16, Ile164, Phe58, Tyr170, Ser108, Ile14, Asp54, Cys15, Leu164, and Met55. Meanwhile, the molecular docking result of chalcones **2a**, **2e**, and **2h** in Table 2 displayed interaction with the common active site residues of the re-docking of the co-crystal inhibitor WR9910. Compounds **2a**, **2e**, and **2h** have functional groups are –OH; halogen substituent (F, Cl, and Br); enolates; amines; and two benzene rings. The –OH group plays an important role in the formation of interaction *via* hydrogen bonds. In addition, the substituted halogen and aminoalkyl groups also take part in the interaction by forming hydrogen bonds. The presence of enolates and benzene rings will result in π-bonds with amino acids in PfDHFR-TS resistance (Fig. 5).

In our previous study, we mentioned that a previously synthesized chalcone derivative with piperidine moiety showed not only *in vitro* activity but also *in silico* computational properties proven by its best hydrogen bond interaction with Ile112, Ile64, Ser111, Ser108, Asp54, Tyr170, and Pro113 residues on PfDHFR-TS (CDOCKER energy = −48.84 kcal mol^{-1}).[32,33] Not only that, the most active compound (*E*)-3-(3,4-dimethoxy phenyl)-1-(2-hydroxy-4-methoxy-5-(prenyl)phenyl)-prop-2-en-1-one was employed in the docking simulation showing perfect binding with amino acids Ala16, Ser108, Ile164, Trp48, and Phe58 in PfDHFR-TS.[11] The *in silico* properties of these synthesized chalcone derivatives **2a**, **2e**, and **2h** on PfDHFR-TS supported the *in vitro* antimalarial effect. A similar effect can be observed in this study where *in silico* properties of chalcone derivatives **2a**, **2e**, and **2h** also corroborated with their *in vitro* antimalarial activities.

Physicochemical properties and ADMET analysis for chalcone derivatives

Investigation of pharmacokinetic parameters is crucial in the evaluation of drug candidates. It has been stated that the development of chalcone derivatives as drug candidates has some issues related to decreased bioavailability, low distribution, accelerated metabolism, and elimination.[40] In this work, further studies related to the drug-likeness and ADMET properties were only carried out on chalcones **2a**, **2e**, and **2h** with

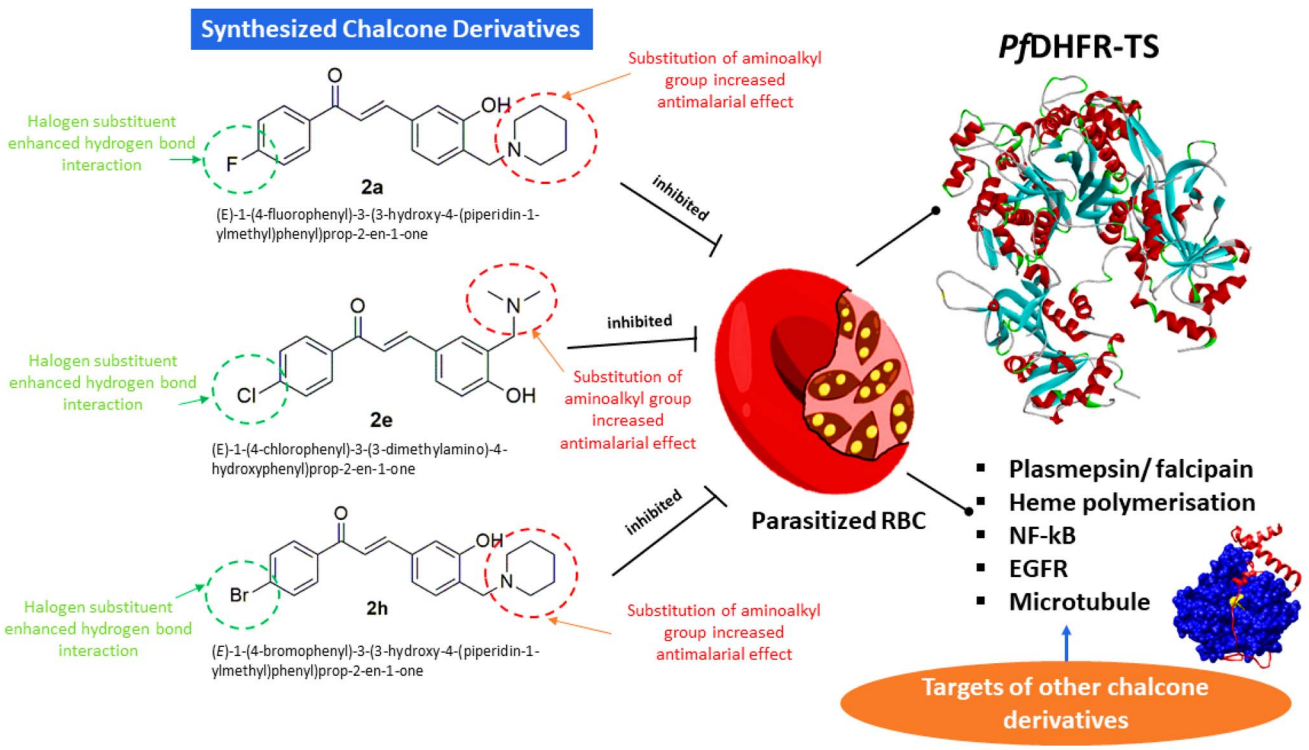

Fig. 5 A plausible mechanism of action of the synthesized chalcone derivatives on malarial parasite.

potential antimalarial activities against *P. knowlesi* and *P. falciparum*. Physicochemical properties of the prepared compounds were revealed by following the Lipinski rule based on the molecular weight (MW), number of hydrogen bond acceptors (nHA), number of hydrogen bond donors (nHD), and the logarithm of the *n*-octanol/water distribution (log *P*). Therefore, without any violations of the Lipinski rule, chalcone **2a**, **2e**, and **2h** were predicted to be orally bioavailable. Nevertheless, log *P* values that indicate lipophilicity parameters were considered to be higher than the optimal values (0–3). This result proposes that it could later affect the membrane permeability and hydrophobic binding to macromolecules.

Absorption. The absorption of drugs was predicted based on the membrane permeability showed by human intestinal absorption (HIA), colon cancer cell lines (Caco-2), P-glycoprotein inhibitor, P-glycoprotein substrate, and human oral bioavailability (20% and 30%). Human intestinal absorption (HIA) for an oral drug is important. It can be seen, that chalcone **2a**, **2e**, and **2h** were considered to have good absorption with a prediction score between 0 to 0.3.

The human colon adenocarcinoma cell lines (Caco-2) have been used to predict drug permeability. The prepared chalcones **2a**, **2e**, and **2h** were considered to have a proper Caco-permeability, as they have a predictive value of ≥5.15 log cm s^{-1}. P-glycoprotein (P-gp) is an efflux transmembrane protein

Table 3 Prediction of drug-likeness and ADMET parameters of chalcone derivatives **2a**, **2e**, and **2h**[a]

Parameters	2a	2e	2h
Drug-likeness			
• Molecular weight	339.160	315.100	399.080
• H-bond acceptor	3	3	3
• H-bond donor	1	1	1
• Log *P*	3.982	3.692	4.568
• TPSA	40.540	40.540	40.540
A (absorption)			
• Human intestinal absorption (HIA)	– – (0.012)	– – – (0.005)	– – – (0.021)
• Caco-2 permeability (log cm s^{-1})	−4.889	−4.6	−4.933
• P-glycoprotein inhibitor	– (0.488)	– – – (0.017)	++ (0.786)
• P-glycoprotein substrate	– – – (0.001)	– – – (0.002)	– – – (0.001)
• $F_{20\%}$	– – (0.293)	– – – (0.001)	– – – (0.009)
• $F_{30\%}$	– (0.467)	– – – (0.000)	– – – (0.042)
D (distribution)			
• Plasma protein binding (PPB) (%)	98.109	96.399	97.796
• Blood–brain barrier penetration (BBB) (cm s^{-1})	+ (0.502)	+ (0.604)	– (0.478)
• Volume distribution (L kg^{-1})	1.274	2.128	1.334
• Fu (%)	1.869	3.275	1.535
M (metabolism)			
• CYP1A2 substrate	+ (0.687)	+++ (0.867)	– (0.356)
• CYP1A2 inhibitor	++ (0.759)	++ (0.960)	++ (0.817)
• CYP2C19 substrate	– – – (0.066)	++ (0.765)	– – – (0.069)
• CYP2C19 inhibitor	+ (0.591)	– (0.308)	++ (0.757)
• CYP2C9 substrate	– (0.353)	– (0.455)	– (0.375)
• CYP2C9 inhibitor	– – (0.137)	– – – (0.065)	– – (0.156)
• CYP2D6 substrate	+++ (0.912)	+++ (0.926)	+++ (0.906)
• CYP2D6 inhibitor	+++ (0.960)	+++ (0.969)	+++ (0.970)
• CYP3A4 substrate	– – (0.255)	– (0.445)	– – (0.254)
• CYP3A4 inhibitor	– – (0.183)	– – – (0.047)	– – (0.172)
E (excretion)*			
• Half-time ($t_{1/2}$)	0.093	0.612	0.128
• Clearance (mL min^{-1} kg^{-1})	11.936	12.620	4.691
T (toxicity)			
• Human hepatotoxicity (H-HT)	– (0.330)	+ (0.512)	– – (0.126)
• hERG blockers	+++ (0.978)	– (0.426)	+++ (0.980)
• Rat oral acute toxicity	++ (0.734)	+ (0.562)	– (0.327)
• AMES toxicity	– – (0.108)	– – (0.174)	– – – (0.044)
• Drug-induced liver injury (DILI)	++ (0.723)	++ (0.851)	++ (0.857)
• Carcinogenicity	– (0.350)	– – (0.184)	– – (0.278)
• Acute oral toxicity (kg mol^{-1})*	2.751	2.723	2.765

[a] The symbol * indicates prediction using admetSAR 2.0 (**https://lmmd.ecust.edu.cn/admetsar2/**, accessed on 1 January 2022).

that is partly responsible for the clearance of medicines through the hepatic and renal systems. The transport system of this protein is possible to be induced or inhibited and might lead to the interaction of medicine–medicine and medicine–food. Therefore, it is important to assess the P-gp parameter, both for the inhibitory and substrate of a compound in drug discovery. According to Table 3, chalcone derivatives **2a**, **2e**, and **2h** were predicted to be a non-substrate of the P-glycoprotein (P-gp). In addition, only chalcone **2h** was the P-gp inhibitor.

Human oral bioavailability was assessed for both in 20 and 30%. Theoretically, bioavailability is presented as 100% when a medication is administered straight into the bloodstream and is usually completely used by the body.[41] However, an orally administrated drug might have decreased bioavailability. Chalcone derivatives **2e** and **2h** were predicted to have a good result by showing bioavailability $\geq$ 20 and 30% with predictive values in the range of 0–0.3. Meanwhile, chalcone derivative **2a** was assessed to have good bioavailability of $\geq$20% and moderate bioavailability of 30% (in the range of 0.3–0.7).

Distribution. The distribution of the drugs was predicted based on the plasma protein binding (PBB), volume distribution (VD), blood–brain barrier (BBB) penetration, and the fraction unbound in plasma (Fu) parameters. Plasma protein binding (PPB) is related to the drug uptake and distribution that might affect the oral bioavailability where the free concentration of the drug could decrease because a drug binds to serum proteins. Table 3 shows that the prepared chalcone derivatives **2a**, **2e**, and **2h** were classified as having poor PPB properties as they have a predicted value of $\geq$90%.

The ADMET analysis showed that chalcone derivatives **2a**, **2e**, and **2h** were categorized to have medium BBB parameters with an empirical value between 0.3–0.7, indicating a little BBB penetration. Meanwhile, the empirical VD value of chalcone derivatives **2a**, **2e**, and **2h** was in the range of 0.04 to 20 L kg^{-1}, which was classified as good. Theoretically, the VD is needed to explain the *in vivo* distribution of drugs, for example, the tendencies to bind to plasma protein, measurement of the distribution amount in body fluid, or the uptake amount in issues. Lastly, the fraction unbound in plasma (Fu) parameter of chalcone derivatives **2a**, **2e**, and **2h** resulted in less than 5%, indicating a poor unbound state of drugs in plasma.

Metabolism. The metabolism of drugs was evaluated according to the Cytochrome P450 (CYP) substrate or inhibitor to five isozymes of CYP1A2, CYP3A4, CYP2C9, CYP2C19, and CYP2D6. Chalcone derivative **2a** was found to be substrates to CYP1A2 and CYP2D6, as well as inhibitors to CYP1A2, CYP2C19, and CYP2D6. Furthermore, chalcone derivative **2e** was the substrate to CYP1A2, CYP2C19, and CYP2D6, besides the inhibitors to CYP1A2 and CYP2D6. On the other hand, chalcone derivative **2h** was predicted to be the only substrate to CYP2D6, and the inhibitors to CYP1A2, CYP2C19, and CYP2D6.

Excretion. The excretion profile was evaluated based on the total clearance and the half-life ($t_{1/2}$) parameters. Only chalcone derivative **2h** was predicted to have low total clearance as it has a clearance value of 4.691 mL min^{-1} kg^{-1} (<5 mL min^{-1} kg^{-1}). Meanwhile, chalcone derivatives **2a** and **2e** were categorized as moderate clearance with the predicted value in the range of 5 to 15 mL min^{-1} kg^{-1}. Furthermore, chalcone derivatives **2a** and **2h** were classified to have a short half-life (<3 h) with the output value of 0–0.3, while **2e** was predicted to have a longer half-life as it has an empirical value of 0.612.

Toxicology. Prediction of the toxicology properties was performed to several parameters such as hERG blockers, human hepatotoxicity (H-HT), drug-induced liver injury (DILI), Ames toxicity, rat oral acute toxicity, and carcinogenicity. As recorded in Table 3, chalcone derivatives **2e**, **2a**, and **2h** could induce liver injury but they are relatively non-toxic based on the AMES parameter. Generally, chalcone derivative **2e** has lower toxicity than **2a** and **2h** based on the hERG blockers parameter.

Materials and methods

Chemicals and instrumentation

All chemicals were purchased from Sigma-Aldrich, and Merck and used without further purification. All the solvents and reagents used in the synthesis were analysis and synthesis grade. For molecular docking: the protein used for molecular docking studies was the crystal protein of chloroquine-sensitive *Plasmodium falciparum* dihydrofolate reductases-thymidylate synthase (PfDHFR-TS) (PDB ID: 1J3I). This study used a PC with Intel® Core™ i7 CPU M 350 4.54 GHz; RAM 8.00 GB. Molecular docking using Discovery Studio 2016 (Accelrys, San Diego, USA). Melting points of the prepared compounds were determined in an open capillary tube on Electrothermal 9100. The molecular weight of the compounds was determined based on the MS from Shimadzu QP2010S. The ^{1}H- and ^{13}C-NMR spectra were recorded using tetramethylsilane as an internal standard on JEOL JNMECA (500 MHz).

Synthesis procedures

General procedure for the synthesis of chalcone derivates (1a–d). Acetophenone derivatives (4-fluoroacetophenone, 4-chloroacetophenone, or 4-bromoacetophenone; 10 mmol) and benzaldehyde derivatives (4-hydroxybenzaldehyde or 3-hydroxybenzaldehyde; 10 mmol) were dissolved in 25 mL of ethanol in 100 mL three-neck round-bottom reaction flasks containing a stir bar. To this solution, was added 60% aqueous KOH (5 mL). The mixture was stirred at room temperature for 24 hours and monitored using TLC. The reaction was stopped when the starting materials were completely reacted. After the completion of the reaction, the mixture was poured into iced distilled water in a beaker glass and neutralized using HCl 25%. The precipitate formed was then filtered, washed with distilled water, and dried for further purification using column chromatography. The final product was later characterized using NMR and Mass Spectroscopy (MS).

General procedure for the synthesis of chalcone derivatives (2a–h). The synthesis of aminoalkylated chalcone (**2a–h**) was carried out through the Mannich reaction[16] by dissolving chalcone (**1a–d**) (10 mmol) in ethanol (75 mL) until a homogenous solution was obtained. To this solution, 10 mmol of formaldehyde solution (37%) and 10 mmol of aminoalkyl groups were added while stirring at room temperature. The mixture was then

heated and refluxed for 20 hours or until no starting materials remained (monitored by TLC using hexane : ethyl acetate in 3 : 1 ratio). After the completion of the reaction, the solvent was evaporated under a reduced pressure rotary evaporator, and the solid product obtained was purified using column chromatography with hexane : ethyl acetate mixture (0–50% gradient) as the eluent.[32,42]

*(E)-1-(4-Fluorophenyl)-3-(3-hydroxyphenyl)prop-2-en-1-one (**1a**).* Compound **1a** with the molecular formula of $C_{15}H_{11}FO_2$ was produced as an orange-yellow solid with a melting point of 112–113 °C, molecular ion (*m*/*z*) of 242.07, and yield of 35%. ^{1}H-NMR (CD_3OD, 600 MHz) δ (ppm): 7.91 (m, 2H, H-2, H-6), 7.19 (d, J = 9.0 Hz, 2H, H-3, H-5), 7.50 (d, J = 15.6 Hz, 1H, Hα), 7.68 (d, J = 15.6 Hz, 1H, Hβ), 7.17 (m, 1H, H-6′), 7.29 (m, 1H, H-5′), 6.91 (dd, J = 9.6 and J = 1.8 Hz, 1H, H-4′), 7.05 (s, 1H, H-2′), and 4.82 (s, 1H, O–H). ^{13}C-NMR (CD_3OD, 150 MHz) δ (ppm): 135.8 (1C, C-1), 132.6 (2C, C-2, and C-6), 116.7 (2C, C-3, and C-5), 166.4 (1C, C-4/C–F), 121.5 (1C, C-α), 146.9 (1C, C-β), 191.1 (1C, C=O), 137.4 (1C, C-1′), 122.6 (1C, C-2′), 131.2 (1C, C-3′), 119.4 (1C, C-4′), 159.4 (1C, C-5′), and 116.9 (1C, C-6′).

*(E)-1-(4-Fluorophenyl)-3-(4-hydroxyphenyl)prop-2-en-1-one (**1b**).* Compound **1b** with the molecular formula of $C_{15}H_{11}FO_2$ was obtained as a bright yellow solid with a melting point of 149.2–151 °C, molecular ion (*m*/*z*) of 242.25, and yield of 80%. ^{1}H-NMR (CD_3OD, 600 MHz) δ (ppm): 7.92 (d, J = 8.4 Hz, 2H, H-2, H-6), 7.17 (m, 2H, H-3, H-5), 7.40 (d, J = 15 Hz, 1H, Hα), 7.63 (d, J = 15 Hz, 1H, Hβ), 7.49 (m, 2H, H-2′, H-6′), 6.87 (d, J_1 = 9.0 Hz, 2H, H-3′, H-5′), and 9.95 (s, 1H, O–H). ^{13}C-NMR (CD_3OD, 150 MHz) δ (ppm): 134.7 (1C, C-1), 131.3 (2C, C-2, C-6), 115.6 (2C, C-3, C-5), 166.3 (1C, C-4/C–F), 122.3 (1C, C-α), 144.1 (1C, C-β), 185.4 (1C, C=O), 138.1 (1C, C-1′), 122.1 (2C, C-2′, C-6′), 116.5 (2C, C-3′, C-6′), and 158.2 (1C, C-4′).

*(E)-1-(4-Chlorophenyl)-3-(4-hydroxyphenyl)prop-2-en-1-one (**1c**).* Compound **1c** with the molecular formula of $C_{15}H_{11}ClO_2$ was afforded a bright yellow solid with a melting point of 135.3–137.8 °C, molecular ion (*m*/*z*) of 258.04, and yield of 78%. ^{1}H-NMR ($CDCl_3$, 500 MHz) δ (ppm): 7.99 (d, J = 8.4 Hz, 2H, H-2, H-6), 7.52 (m, 2H, H-3, H-5), 7.40 (d, J = 15 Hz, 1H, Hα), 7.63 (d, J = 15 Hz, 1H, Hβ), 7.49 (m, 2H, H-2′, H-6′), 6.87 (d, J = 9.0 Hz, 2H, H-3′, H-5′), and 9.95 (s, 1H, O–H). ^{13}C-NMR ($CDCl_3$, 125 MHz) δ (ppm): 137.6 (1C, C-1), 131.0 (2C, C-2, C-6), 129.7 (2C, C-3, C-5), 139.1 (1C, C-4/C–Cl), 120.4 (1C, C-α), 144.9 (1C, C-β), 188.7 (1C, C=O), 127.7 (1C, C-1′), 129.5 (2C, C-2′, C-6′), 116.4 (2C, C-3′, C-5′), and 159.9 (1C, C-4′).

*(E)-1-(4-Chlorophenyl)-3-(3-hydroxyphenyl)prop-2-en-1-one (**1d**).* Compound **1d** with the molecular formula of $C_{15}H_{11}ClO_2$ was obtained as a brownish yellow solid with a melting point of 135.2–137.9 °C, molecular ion (*m*/*z*) of 258.70, and yield of 67%. ^{1}H-NMR ($CDCl_3$, 500 MHz) δ (ppm): 7.46 (m, 2H, H-2, H-6), 8.04 (d, J = 9.0 Hz, 2H, H-3, H-5), 7.74 (d, J = 15 Hz, 1H, Hα), 8.02 (d, J = 15 Hz, 1H, Hβ), 7.28 (m, 1H, H-2′), 7.10 (brs, 1H, H-3′), 7.02 (m, 1H, H-4′), 7.00 (m, 1H, H-6′), and 4.84 (s, 1H, O–H). ^{13}C-NMR ($CDCl_3$, 125 MHz) δ (ppm): 136.7 (1C, C-1), 130.0 (2C, C-2, C-6), 129.1 (2C, C-3, C-5), 139.2 (1C, C-4/C–Cl), 121.2 (1C, C-α), 145.6 (1C, C-β), 189.4 (1C, C=O), 135.3 (1C, C-1′), 124.9 (1C, C-2′), 131.2 (1C, C-3′), 125.0 (1C, C-4′), 158.6 (1C, C-5′), and 115.0 (1C, C-6′).

*(E)-1-(4-Fluorophenyl)-3-(3-hydroxy-4-(piperidin-1-ylmethyl) phenyl)prop-2-en-1-one (**2a**).* Compound **2a** with the molecular formula of $C_{21}H_{22}FNO_2$ was obtained as a yellow solid with a melting point of 155–156 °C, and a yield of 85%. ^{1}H-NMR ($CDCl_3$, 500 MHz) δ (ppm): 7.97 (m, 2H, H-2, H-6), 7.09 (d, J = 9.0 Hz, 2H, H-3, H-5), 7.39 (d, J = 15.6 Hz, 1H, Hα), 7.65 (d, J = 15.6 Hz, 1H, Hβ), 7.24 (m, 1H, H-2′), 7.03 (m, 1H, H-6′), 7.05 (m, 1H, H-3′), 4.84 (s, 1H, O–H), 3.68 (s, 2H, CH_2), and 1.66–1.13 (m, 10H, H-2″, H-3″, H-4″, H-5″, H-6″). ^{13}C-NMR ($CDCl_3$, 125 MHz) δ (ppm): 134.6 (1C, C-1), 131.1 (2C, C-2, C-6), 115.7 (2C, C-3, C-5), 165.6 (1C, C-4/C–F), 192.2 (1C, C=O), 120.1 (1C, C-α), 158.9 (1C, C-β), 158.5 (1C, C-1′), 115.1 (1C, C-2′), 188.9 (1C, C-3′), 120.5 (1C, C-4′), 121.3 (1C, C-5′), 116.8 (1C, C-6′), and 53.9–23.7 (**C**H_2, C-2″, C-3″, C-4″, C-5″, C-6″).

*(E)-1-(4-Fluorophenyl)-3-(4-hydroxy-3-(morpholinomethyl) phenyl)prop-2-en-1-one (**2b**).* Compound **2b** with the molecular formula of $C_{20}H_{20}FNO_3$ and molecular ion (*m*/*z*) of 341.38 was obtained as a brown solid, and a yield of 52%. ^{1}H-NMR ($CDCl_3$, 500 MHz) δ (ppm): 7.96 (m, 2H, H-2, H-6), 7.24 (m, 2H, H-3, H-5), 7.42 (d, J = 15 Hz, 1H, Hα), 7.76 (d, J = 15 Hz, 1H, Hβ), 7.48 (m, 1H, H-2′), 6.85 (d, J = 5 Hz, 1H, H-3′), 7.29 (m, 1H, H-6′), 4.84 (s, 1H, O–H), 3.71 (s, 2H, CH_2), 2.67 (m, 2H, H-2″, H-6″), and 3.69 (m, 2H, H-3″, H-5″). ^{13}C-NMR ($CDCl_3$, 125 MHz) δ (ppm): 134.7 (1C, C-1), 131.3 (2C, C-2, C-6), 115.9 (2C, C-3, C-5), 165.4 (1C, C-4/C–F), 122.2 (1C, C-α), 144.7 (1C, C-β), 190.2 (1C, C=O), 127.0 (1C, C-1′), 130.0 (1C, C-2′), 126.6 (1C, C-3′), 157.2 (1C, C-4′), 116.2 (1C, C-5′), 131.3 (1C, C-6′), 59.6 (**C**H_2), 54.2 (2C, C-2″, C-6″), and 66.4 (2C, C-3″, C-5″).

*(E)-1-(4-Fluorophenyl)-3-(4-hydroxy-3-(piperidin-1-ylmethyl) phenyl)prop-2-en-1-one (**2c**).* Compound **2c** with the molecular formula of $C_{21}H_{22}FNO_2$ and molecular ion (*m*/*z*) of 339.41 was afforded as a light brown solid, and yield of 82%. ^{1}H-NMR ($CDCl_3$, 500 MHz) δ (ppm): 8.05 (d, J = 8.4 Hz, 2H, H-2, H-6), 7.17 (m, 2H, H-3, H-5), 7.34 (d, J = 15 Hz, 1H, Hα), 7.75 (d, J = 15 Hz, 1H, Hβ), 7.50 (m, 2H, H-2′, H-6′), 6.85 (d, J = 10 Hz, 1H, H-3′), 7.28 (m, 1H, H-6′), 4.84 (s, 1H, O–H), 3.73 (s, 2H, CH_2), and 2.51–1.25 (10H, H-2″, H-3″, H-4″, H-5″, H-6″). ^{13}C-NMR ($CDCl_3$, 125 MHz) δ (ppm): 134.9 (1C, C-1), 130.9 (2C, C-2, C-6), 115.6 (2C, C-3, C-5), 166.4 (1C, C-4/C–F), 118.2 (1C, C-α), 145.4 (1C, C-β), 188.8 (1C, C=O), 125.8 (1C, C-1′), 129.5 (2C, C-2′, C-6′), 122.0 (1C, C-3′), 161.3 (1C, C-4′), 116.8 (1C, C-5′), 61.9 (1C, C-1″), 53.8 (2C, C-2″, C-6″), 23.8 (1C, C-4″), and 25.7 (2C, C-3″, C-5″).

*(E)-1-(4-Fluorophenyl)-3-((4-hydroxy-3-(4-methylpiperidin-1-yl) methyl)phenyl)prop-2-en-1-one (**2d**).* Compound **2d** with the molecular formula of $C_{22}H_{24}FNO_2$ and molecular ion (*m*/*z*) of 353.44 was produced as a dark yellow solid, and a yield of 75%. ^{1}H-NMR ($CDCl_3$, 500 MHz) δ (ppm): 8.05 (d, J = 8.4 Hz, 2H, H-2, H-6), 7.15 (m, 2H, H-3, H-5), 7.43 (d, J = 15 Hz, 1H, Hα), 7.75 (d, J = 15 Hz, 1H, Hβ), 7.50 (m, 2H, H-2′, H-6′), 6.84 (d, J = 10 Hz, 1H, H-3′), 4.84 (s, 1H, O–H), 3.73 (s, 2H, CH_2), 2.97–1.72 (m, 10H, H-2″, H-3″, H-4″, H-5″, H-6″), and 1.30 (m, 3H, CH_3). ^{13}C-NMR ($CDCl_3$, 125 MHz) δ (ppm): 134.9 (1C, C-1), 130.9 (2C, C-2, C-6), 115.6 (2C, C-3, C-5), 166.6, 164.4 (1C, C-4/C–F), 122.0 (1C, C-α), 145.4 (1C, C-β), 188.8 (1C, C=O), 129.2 (1C, C-1′), 130.6 (1C, C-2′), 125.8 (1C, C-3′), 161.3 (1C, C-4′), 116.8 (1C, C-5′), 129.5

(1C, C-6′), 61.5 (1C, C-1″), 53.3 (2C, C-2″, C-6″), 34.0 (2C, C-3″, C-5″), 30.4 (1C, C-4″), and 21.6 (1C, CH_3).

*(E)-1-(4-Chlorophenyl)-3-(3-dimethylamino)-(4-hydroxyphenyl) prop-2-en-1-one (**2e**).* Compound **2e** with the molecular formula of $C_{17}H_{16}ClNO_2$ and molecular ion (*m*/*z*) of 301.77 was produced as a brown solid with a yield of 82%. ^{1}H-NMR ($CDCl_3$, 500 MHz) δ (ppm): 7.96 (m, 2H, H-2, H-6), 7.42 (m, 2H, H-3, H-5), 7.45 (d, J = 15 Hz, 1H, Hα), 7.76 (d, J = 15 Hz, 1H, Hβ), 6.94 (m, 1H, H-2′), 6.70 (d, J = 10 Hz, 1H, H-3′), 7.48 (m, 1H, H-6′), 4.84 (s, 1H, O–H), 3.75 (s, 2H, CH_2), and 2.35 (s, 6H, CH_3). ^{13}C-NMR ($CDCl_3$, 125 MHz) δ (ppm): 136.6 (1C, C-1), 130.6 (2C, C-2, C-6), 129.7 (2C, C-3, C-5), 138.8 (1C, C-4/C–Cl), 122.3 (1C, C-α), 145.8 (1C, C-β), 189.3 (1C, C═O), 126.6 (1C, C-1′), 130.6 (1C, C-2′), 125.7 (1C, C-3′), 161.3 (1C, C-4′), 116.9 (1C, C-5′), 128.9 (1C, C-6′), 44.4 (3C, CH_3), and 62.5 (1C, CH_2).

*(E)-1-(4-Chlorophenyl)-3-(4-hydroxy-3-((4-methylpiperidin-1-yl) methyl)phenyl)prop-2-en-1-one (**2f**).* Compound **2f** with the molecular formula of $C_{22}H_{24}ClNO_2$ and molecular ion (*m*/*z*) of 369.89 was obtained as a brick red solid with a yield of 76%. ^{1}H-NMR ($CDCl_3$, 500 MHz) δ (ppm): 7.96 (d, J = 8.4 Hz, 2H, H-2, H-6), 7.49 (m, 2H, H-3, H-5), 7.32 (d, J = 15 Hz, 1H, Hα), 7.76 (d, J = 15 Hz, 1H, Hβ), 7.51 (m, 2H, H-2′, H-6′), 6.85 (d, J = 10 Hz, 1H, H-3′), 4.84 (s, 1H, O–H), 3.74 (s, 2H, CH_2), 2.98–3.0 (m, 2H, H-2″, H-6″), 1.33–1.71 (m, 2H, H-3″, H-5″), 2.14 (m, 1H, H-4″), and 1.31 (s, 3H, CH_3). ^{13}C-NMR ($CDCl_3$, 125 MHz) δ (ppm): 137.9 (1C, C-1), 129.8 (2C, C-2, C-6), 129.3 (2C, C-3, C-5), 138.8 (1C, C-4/C–Cl), 122.0 (1C, C-α), 145.7 (1C, C-β), 189.2 (1C, C═O), 129.3 (1C, C-1′), 129.8 (1C, C-2′), 129.6 (1C, C-6′), 128.8 (1C, C-3′), 116.8 (1C, C-5′), 61.5 (1C, C-1″), 53.0 (2C, C-2″, C-6″), 34.0 (2C, C-3″, C-5″), 30.0 (1C, C-4″), and 21.5 (3C, CH_3).

*(E)-1-(4-Chlorophenyl)-3-(3-hydroxy-4-((4-methylpiperidin-1-yl) methyl)phenyl)prop-2-en-1-one (**2g**).* Compound **2g** with the molecular formula of $C_{22}H_{24}ClNO_2$ and molecular ion (*m*/*z*) of 369.89 was obtained as a brick red solid with a yield of 75%. ^{1}H-NMR ($CDCl_3$, 500 MHz) δ (ppm): 7.96 (d, J = 3.51 Hz, 2H, H-2, H-6), 7.49 (d, J = 10 Hz, 2H, H-3, H-5), 7.32 (d, J = 15 Hz, 1H, Hα), 7.76 (d, J = 15 Hz, 1H, Hβ), 7.51 (m, 1H, H-2′), 6.85 (d, J = 10 Hz, 1H, H-3′), 6.92 (d, J = 5 Hz, 1H, H-6′), 4.84 (s, 1H, O–H), 3.74 (s, 2H, CH_2), 2.98–3.0 (m, 2H, H-2″, H-6″), 1.33–1.71 (m, 2H, H-3″, H-5″), 2.14 (m, 1H, H-4″), and 1.31 (s, 3H, CH_3). ^{13}C-NMR ($CDCl_3$, 125 MHz) δ (ppm): 137.9 (1C, C-1), 129.8 (2C, C-2, C-6), 129.3 (2C, C-3, C-5), 138.8 (1C, C-4/C–Cl), 122.0 (1C, C-α), 145.7 (1C, C-β), 189.2 (1C, C═O), 129.3 (1C, C-1′), 129.8 (1C, C-2′), 129.6 (1C, C-6′), 128.8 (1C, C-3′), 116.8 (1C, C-5′), 61.5 (1C, C-1″), 53.0 (2C, C-2″, C-6″), 34.0 (2C, C-3″, C-5″), 30.0 (1C, C-4″), and 21.5 (3C, CH_3).

*(E)-1-(4-Bromophenyl)-3-(3-hydroxy-4-(piperidin-1-ylmethyl) phenyl)prop-2-en-1-one (**2h**).* Compound **2h** with the molecular formula of $C_{21}H_{22}BrNO_2$ and molecular ion (*m*/*z*) of 399.83 was produced as a bright yellow amorphous solid, and a yield of 89%. ^{1}H-NMR ($CDCl_3$, 500 MHz) δ (ppm): 7.81 (d, J = 8.5 Hz, 2H, H-2, H-6), 7.77 (d, J = 15.6 Hz, 1H, Hβ), 7.57 (m, 2H, H-3′, H-5′), 7.34 (d, J = 15.6 Hz, 1H, Hα), 7.04 (m, 1H, H-2′), 6.96 (m, 1H, H-6′), 4.84 (s, 1H, O–H), 3.63 (s, 2H, CH_2), and 2.61–1.58 (m, 10H, H-2″, H-3″, H-4″, H-5″, H-6″). ^{13}C-NMR ($CDCl_3$, 125 MHz) δ (ppm): 189.4 (1C, C-1), 131.9 (2C, C-2, C-6), 130.0 (C-3, C-5), 129.0 (C-4/C–Br), 120.1 (1C, C-α), 158.9 (1C, C-β), 135.1 (1C, C-1′), 115.0 (1C, C-2′), 158.6 (1C, C-3′), 124.9 (1C, C-4′), 131.8 (1C, C-5′), 120.2 (1C, C-6′), 62.0 (CH_2), 54.0 (C-2″, C-6″), 25.8 (C-3″, C-5″), and 23.9 (C-4″).

Antimalarial assay of chalcone derivatives using *in vitro P. knowlesi* A1H1 and *P. falciparum* 3D7 cultures

Plasmodium knowlesi A1H1 strain was collected from Malaria Culture Laboratory, Department of Parasitology, Faculty of Medicine, Universiti Malaya (contributed by Robert W. Moon, London School of Hygiene and Tropical Medicine, London, UK) and *P. falciparum* 3D7 (chloroquine-sensitive) (MRA-102) were originally obtained from BEI Resources, NIAID, NIH (*P. falciparum*, strain 3D7, MRA-102, contributed by Daniel J. Carucci). The parasites were cultivated in fresh human blood (group O rhesus positive) suspended in RPMI 1640 (Invitrogen Life Technologies, NY, USA) supplemented with glucose (3 g L^{-1}), hypoxanthine (45 μg L^{-1}), and gentamicin (50 μg L^{-1}). *Plasmodium knowlesi* was cultivated in RPMI 1640 medium supplemented with 10% horse serum (Gibco, New Zealand)[43] and *P. falciparum* culture medium was supplemented with 10% AlbuMAX I as described by Trager and Jensen.[44] *Plasmodium* lactate dehydrogenase (pLDH) assays for *P. knowlesi* and *P. falciparum* were performed based on a method by Makler and Hinrichs[45] with slight modifications.[46,47] Parasites (2% hematocrit and 2% parasitemia) were cultivated in a synchronized phase in 96-well plates. A total of 1 μL of the test compound in various concentrations was added with 99 μL of the parasite culture. Parasitized red blood cells (no treatment) were set as the controls while unparasitized red blood cells (no treatment) were set as the blanks in the assay. Chloroquine diphosphate served as a reference drug in the assay. The well plate was then put into the chamber and given mixed gas (O_2 5%, CO_2 5%, and N_2 90%) and incubated for 24 hours at 37 °C for *P. knowlesi* and 72 hours at 37 °C for *P. falciparum*. Afterward, the plates were frozen at −20 °C for 24 hours and thawed at 37 °C for 30 minutes to lyse the red blood cells. Malstat reagent (100 μL) and nitro blue tetrazolium salt/phenazine ethosulfate (NBT/PES) (25 μL) were added to a new plate containing the treated cultures (25 μL). The color development of the plates was monitored at 650 nm using a SpectraMax Paradigm® Multi-Mode microplate reader. Data were analyzed through a non-linear regression *via* GraphPad Prism software to obtain EC_{50} values (half-maximal effective concentration).

Cytotoxicity assay of chalcone derivatives using *in vitro* WRL-68 mammalian cell line

A human normal liver WRL68 cell line (ATCC: CL-48) was purchased from the American Type Culture Collection (ATCC).[48] The cell lines were cultivated in MEM medium (supplemented with 5% of FBS and 1% of penicillin–streptomycin) in a tissue culture flask (T25) (Nunc, USA) at 37 °C and 5% CO_2 in a sterile incubator. The culture medium was changed every day until cells became confluent and ready to be sub-culture. When the cells reached confluency, the media were removed and washed with phosphate buffer saline (PBS, Gibco, USA). Cells were detached by adding trypsin (Gibco, USA) and incubated for 5–10

minutes at 37 °C. The cell suspension was transferred into a 15 mL sterile tube and centrifuged at 300 g for 5 minutes. The cells were resuspended in a culture medium and maintained in a continuous culture before being used for the cytotoxic assay.

The WRL-68 cell lines were used in the colorimetric assay of 3-(4,5-dimethylthiazol-2-yl)-2,5-diphenyl-tetrazolium bromide (MTT) to study *in vitro* cytotoxicity activity.[49] About 100 μL cell suspension (5×10^4 cells) were seeded in 96-well microplates for 24 hours. The culture medium was removed from each well and 200 μL of complete medium was added. The cells then were treated with 2 μL of chalcone derivatives diluted in dimethyl sulfoxide (DMSO) at various concentrations (3–990 μM). After 72 hours of incubation at 37 °C, the medium was discarded, and the treated cells were mixed with 20 μL of MTT solution (5 mg mL^{-1}). Absorbance was recorded at 570 nm using enzyme-linked immune sorbent assay (ELISA) SpectraMax Paradigm® Multi-Mode plate reader. Cell viability (%) was determined using the following formula:

$$\text{Cell viability (\%)} = \frac{\text{absorbance of treated cells}}{\text{absorbance of control}} \times 100\%$$

IC_{50} values (inhibition concentration at 50% cell growth) were measured from a non-linear regression using GraphPad Prism software.

Selectivity indexes calculation

The selectivity index (SI) was calculated as the ratio between the inhibitory activity against the normal liver cell line (IC_{50} WRL-68) and the *Plasmodium* parasites, *P. knowlesi* (EC_{50} PkA1H1) or *P. falciparum* (EC_{50} Pf3D7). The SI value is calculated based on the formula *i.e.* SI = (IC_{50} for normal cell line WRL-68)/(EC_{50} for *Plasmodium* spp.). The higher SI value (SI > 10) for a test compound theoretically indicates the effectiveness and safety of a drug.[50–53]

Molecular docking

Molecular docking analysis of the synthesized chalcone derivatives **2a**, **2e**, and **2h** on PfDHFR-TS was conducted referring to the standard docking protocol CDOCKER method from Discovery Studio software.[32] Molecular docking was carried out toward the crystal protein structure of the CQ-sensitive *Plasmodium falciparum* dihydrofolate reductase-thymidylate synthase (PfDHFR-TS) with Protein Database Bank (PDB) ID of IJ3I (resolution of 2.33 Å) (**https://www.rcsb.org**, accessed on 1 January 2022). Before the analysis, the ligands and the receptor protein were constructed using Discovery Studio software. Hydrogen atoms were added to the protein molecule, and the pH of the ionizable amino acids (residues) was adjusted to 7.4. The receptor was maintained rigid during the docking analysis. The docking tolerance of the ligand–receptor was set as 0.25 Å with a few nonpolar or polar hotspots in the receptor. The conformations of the ligands were set at 500 within the relative energy threshold of 20.[54]

ADMET parameters

The physicochemical and pharmacokinetic analysis *i.e.* absorption, distribution, metabolism, excretion, and toxicology (ADMET) parameters were predicted using the online webserver of admetSAR 2.0 (**https://lmmd.ecust.edu.cn/admetsar2/admetopt/**, accessed on 1 January 2022)[55] and ADMETlab 2.0 (**https://admetmesh.scbdd.com/service/evaluation/index**, assessed on 1 January 2022).[56] Drug-like properties were assessed based on the prediction of Lipinski's 'rule of 5' including molecular weight (MW) < 500 g mol^{-1}, number of hydrogen bond acceptors (nHA) ≤ 10, number of hydrogen bond donors (nHD) ≤ 5, and the logarithm of the *n*-octanol/water distribution ($\log P$) ≤ 5.[57] Lipinski's rule predicts that if molecules have two or more violations of the rules, consequently they would potentially not be orally bioavailable as a drug (unacceptable). Meanwhile, the parameters of the absorption, distribution, metabolism, excretion, and toxicology properties are listed in Table 3.

Conclusions

The results of this study indicated that the addition of aminoalkyl groups to chalcone derivatives can increase the antimalarial activity of chalcone Mannich-type base derivatives. The best antimalarial activities were shown by compounds **2a**, **2e**, and **2h** against *P. knowlesi* and *P. falciparum*. The results of *in vitro* antimalarial activities were also supported by the results of analysis using molecular docking suggesting that PfDHFR-TS is a promising target for these compounds. Thus, the findings in this study suggest that the substitution of the amine group in chalcone derivatives is crucial as an alternative therapy to combat drug resistance in *P. falciparum* and the high incidence of malarial infection in *P. knowlesi*. However, *in vivo* trials need to be carried out to further verify the antimalarial action and mechanism of these chalcone derivatives. This study may provide insights into alternative drug discovery efforts to combat antifolate resistance and malaria transmission worldwide.

Author contributions

Conceptualization, JS, JL; methodology, JS, AHA, NYL, NI; investigation, JS, AHA, NYL, NI, RH, NL, BAN; data curation, JS, HKA, LYL, JL, BAN; writing—original draft preparation, JS, AHA, JL; writing—review and editing, JS, JL, HKA; supervision, JS, HKA, JL, LYL; funding acquisition, JS, JL. All authors have read and agreed to the published version of the manuscript.

Conflicts of interest

There are no conflicts to declare.

Acknowledgements

The financial assistance from the Deputy of Research and Development Strengthening of The Ministry of Education, Culture, Research, and Technology/National Agency for

Research and Innovation through LLDIKTI Region X with grant number 074/LL10/PG-PDTT/2021 is highly appreciated and Universiti Kebangsaan Malaysia (GUP-2021-047). We appreciate the great support from the staff and students from the Department of Parasitology, Faculty of Medicine, University of Malaya.

Notes and references

1 World Health Organization (WHO), *World Malaria Report*, Geneva, 2022, **https://www.who.int/teams/global-malaria-programme/reports/world-malaria-report-2022**.
2 Ministry of Health (MOH), *Tren Kasus Malaria Menurun*, Indonesia, 2022, **https://www.kemkes.go.id/article/view/21042300004/tren-kasus-malaria-menurun.html**, accessed on 30 June 2022.
3 N. J. Spillman, R. J. Allen, C. W. McNamara, B. K. Yeung, E. A. Winzeler, T. T. Diagana and K. Kirk, *Cell Host Microbe*, 2013, **13**, 227–237.
4 E. A. Ashley, M. Dhorda, R. M. Fairhurst, C. Amaratunga, P. Lim, S. Suon, S. Sreng, J. M. Anderson, S. Mao and B. Sam, *N. Engl. J. Med.*, 2014, **371**(5), 411–423.
5 C. H. Sibley, *Science*, 2015, **347**, 373–374.
6 B. Sharma, P. Singh, A. K. Singh and S. K. Awasthi, *Eur. J. Med. Chem.*, 2021, **219**, 113408.
7 P. Singh, C. Sharma, B. Sharma, A. Mishra, D. Agarwal, D. Kannan, J. Held, S. Singh and S. K. Awasthi, *Eur. J. Med. Chem.*, 2022, **244**, 114774.
8 P. Yadav, B. Sharma, C. Sharma, P. Singh and S. K. Awasthi, *ACS Omega*, 2020, **5**(12), 6472–6480.
9 N. Chaianantakul, R. Sirawaraporn and W. Sirawaraporn, *Malar. J.*, 2013, **12**(1), 1–13.
10 R. Reeta, V. Rajendran, T. M. Rangarajan, R. P. Ayushee Singh and M. Singh, *Bioorg. Chem.*, 2019, **86**, 631–640.
11 J. Syahri, K. Rullah, R. Armunanto, E. Yuanita, B. A. Nurohmah, M. F. F. Mohd Aluwi, L. K. Wai and B. Purwono, *Asian Pac. J. Trop. Dis.*, 2017, **7**, 9–14.
12 H.-L. Qin, Z.-W. Zhang, R. Lekkala, H. Alsulami and K. Rakesh, *Eur. J. Med. Chem.*, 2020, **193**, 112215.
13 H. Suwito, J. Jumina, M. Mustofa, P. Pudjiastuti, M. Z. Fanani, Y. Kimata-Ariga, R. Katahira, T. Kawakami, T. Fujiwara, T. Hase, H. M. Sirat and N. N. Puspaningsih, *Molecules*, 2014, **19**, 21473–21488.
14 R. Jyoti, R. Gaur, Y. Kumar, H. S. Cheema, D. S. Kapkoti, M. P. Darokar, F. Khan and R. S. Bhakuni, *Nat. Prod. Res.*, 2021, **35**(19), 3261–3268.
15 N. Tadigoppula, V. Korthikunta, S. Gupta, P. Kancharla, T. Khaliq, A. Soni, R. K. Srivastava, K. Srivastava, S. K. Puri, K. S. R. Raju, D. Wahajuddin, P. S. Sijwali, V. Kumar and I. S. Mohammad, *J. Med. Chem.*, 2013, **56**, 31–45.
16 A. Wilhelm, P. Kendrekar, A. E. M. Noreljaleel, E. T. Abay, S. L. Bonnet, L. Wiesner, C. de Kock, K. J. Swart and J. H. Westhuizen, *J. Nat. Prod.*, 2015, **78**, 1848–1858.
17 B. Ngameni, K. Cedric, A. T. Mbaveng, M. Erdoğan, I. Simo, V. Kuete and A. Daştan, *Bioorg. Med. Chem. Lett.*, 2021, **35**, 127827.
18 B. Rioux, A. Pinon, A. Gamond, F. Martin, A. Laurent, Y. Champavier, C. Barette, B. Liagre, C. Fagnere and V. Sol, *Eur. J. Med. Chem.*, 2021, **222**, 113586.
19 S. Sivapriya, K. Sivakumar and H. Manikandan, *Chem. Data Collect.*, 2021, **35**, 100762.
20 H. Ur-Rashid, Y. Xu, N. Ahmad, Y. Muhammad and L. Wang, *Bioorg. Chem.*, 2019, **87**, 335–365.
21 L. Wang, X. Yang, Y. Zhang, R. Chen, Y. Cui and Q. Wang, *J. Nat. Prod.*, 2019, **82**, 2761–2767.
22 W. Dan and J. Dai, *Eur. J. Med. Chem.*, 2020, **187**, 111980.
23 T. S. Freitas, J. C. Xavier, R. L. Pereira, J. E. Rocha, F. F. Campina, J. B. de Araújo Neto, M. M. Silva, C. R. Barbosa, E. S. Marinho and C. E. Nogueira, *Microb. Pathog.*, 2021, **161**, 105286.
24 M. A. Garcia, R. S. Theodoro, J. C. Sardi, M. B. Santos, G. M. Ayusso, F. R. Pavan, A. R. Costa, L. M. Santa Cruz, P. L. Rosalen and L. O. Regasini, *Bioorg. Chem.*, 2021, **116**, 105279.
25 S. K. Konidala, V. Kotra, R. C. S. R. Danduga, P. K. Kola, R. R. Bhandare and A. B. Shaik, *Arabian J. Chem.*, 2021, **14**(6), 103154.
26 G. Prabakaran, S. Manivarman and M. Bharanidharan, *Mater. Today: Proc.*, 2022, **48**, 400–408.
27 A. Rammohan, B. V. Bhaskar, N. Venkateswarlu, W. Gu and G. V. Zyryanov, *Bioorg. Chem.*, 2020, **95**, 103527.
28 T. I. Adelusi, L. Du, A. Chowdhury, G. Xiaoke, Q. Lu and X. Yin, *Life Sci.*, 2021, **284**, 118982.
29 D. Cáceres-Castillo, R. M. Carballo, R. Quijano-Quiñones, G. Mirón-López, M. Graniel-Sabido, R. E. Moo-Puc and G. J. Mena-Rejón, *Med. Chem. Res.*, 2020, **29**, 431–441.
30 D. Quaglio, N. Zhdanovskaya, G. Tobajas, V. Cuartas, S. Balducci, M. S. Christodoulou, G. Fabrizi, M. Gargantilla, E.-M. Priego and A. l. Carmona Pestaña, *ACS Med. Chem. Lett.*, 2019, **10**(4), 639–643.
31 J. Syahri, H. Nasution, B. A. Nurohmah, B. Purwono and E. Yuanita, *J. Appl. Pharm. Sci.*, 2020, **10**, 001–005.
32 J. Syahri, H. Nasution, B. A. Nurohmah, B. Purwono, E. Yuanita, N. H. Zakaria and N. I. Hassan, *Sains Malays.*, 2020, **49**, 2667–2677.
33 M. Mushtaque, *Eur. J. Med. Chem.*, 2015, **90**, 280–295.
34 M. F. Dolabela, S. G. Oliveira, J. M. Nascimento, J. M. Peres, H. Wagner, M. M. Póvoa and A. B. de Oliveira, *Phytomedicine*, 2008, **15**(5), 367–372.
35 K. Katsuno, J. N. Burrows, K. Duncan, R. H. Van Huijsduijnen, T. Kaneko, K. Kita, C. E. Mowbray, D. Schmatz, P. Warner and B. Slingsby, *Nat. Rev. Drug Discovery*, 2015, **14**(11), 751–758.
36 A. H. Ali, H. K. Agustar, N. I. Hassan, J. Latip, N. Embi and H. M. Sidek, *Data Brief*, 2020, **33**, 106592.
37 A. M. Burger and H. H. Fiebig, *Handbook of Anticancer Pharmacokinetics and Pharmacodynamics*, 2014, pp. 23–38.
38 P. Wiji Prasetyaningrum, A. Bahtiar and H. Hayun, *Sci. Pharm.*, 2018, **86**, 25.
39 B. Purwono, B. Nurohmah, P. Fathurrohman and J. Syahri, *Rasayan J. Chem.*, 2021, **14**(1), 94–100.
40 S. Sinha, A. Prakash, B. Medhi, A. Sehgal, D. I. Batovska and R. Sehgal, *BMC Res. Notes*, 2021, **14**, 264.

41 R. Kumar, A. Sharma and P. K. Varadwaj, *J. Nat. Sci., Biol. Med.*, 2011, **2**(2), 168.
42 N. Nurlaili, H. Saputri, S. Z. Nasution, R. Hilma and J. Syahri, *AIP Conf. Proc.*, 2021, **2370**(1), 1–9.
43 A. Amir, B. Russell, J. W. K. Liew, R. W. Moon, M. Y. Fong, I. Vythilingam, V. Subramaniam, G. Snounou and Y. L. Lau, *Sci. Rep.*, 2016, **6**(1), 24623.
44 W. Trager and J. B. Jensen, *Int. J. Parasitol.*, 1997, **27**, 989–1006.
45 M. T. Makler and D. J. Hinrichs, *Am. J. Trop. Med. Hyg.*, 1993, **48**(2), 205–210.
46 S. Nkhoma, M. Molyneux and S. Ward, *Am. J. Trop. Med. Hyg.*, 2007, **76**(6), 1107–1112.
47 M. A. Shamsuddin, A. H. Ali, N. H. Zakaria, M. F. Mohammat, A. S. Hamzah, Z. Shaameri, K. W. Lam, W. F. Mark-Lee, H. K. Agustar and M. R. Mohd Abd Razak, *Pharmaceuticals*, 2021, **14**(11), 1174.
48 American Type Culture Collection (ATCC), Virginia, United States, 2022, **https://www.atcc.org/products/cl-48**, accessed on 1 January 2022.
49 T. Mosmann, *J. Immunol. Methods*, 1983, **65**(1–2), 55–63.
50 D. P. Iwaniuk, E. D. Whetmore, N. Rosa, K. Ekoue-Kovi, J. Alumasa, A. C. de Dios, P. D. Roepe and C. Wolf, *Bioorg. Med. Chem.*, 2009, **17**(18), 6560–6566.
51 S. O. Sarr, S. Perrotey, I. Fall, S. Ennahar, M. Zhao, Y. M. Diop, E. Candolfi and E. Marchioni, *Malar. J.*, 2011, **10**, 1–10.
52 N. H. M. Radzuan, N. A. Z. Norazmi, A. H. Ali and M. Abu, *Sains Malays.*, 2021, **50**(10), 2945–2956.
53 N. A. Z. Norazmi, N. H. Mukhtar, A. H. Ali, N. H. Abd and I. Hassan, *Sains Malays.*, 2022, **51**(4), 1123–1130.
54 J. Yuvaniyama, P. Chitnumsub, S. Kamchonwongpaisan, J. Vanichtanankul, W. Sirawaraporn, P. Taylor, M. D. Walkinshaw and Y. Yuthavong, *Nat. Struct. Mol. Biol.*, 2003, **10**, 357–365.
55 C.-Y. Jia, J.-Y. Li, G.-F. Hao and G.-F. Yang, *Drug Discovery Today*, 2020, **25**(1), 248–258.
56 G. Xiong, Z. Wu, J. Yi, L. Fu, Z. Yang, C. Hsieh, M. Yin, X. Zeng, C. Wu, A. Lu, X. Chen, T. Hou and D. Cao, *Nucleic Acids Res.*, 2021, **49**, w5–w14.
57 C. A. Lipinski, F. Lombardo, B. W. Dominy and P. J. Feeney, *Adv. Drug Delivery Rev.*, 1997, **23**(1–3), 3–25.